Nonuniform rotation and the resistive wall mode

C. G. Gimblett, R. J. Hastie, R. A. M. Van der Linden, and J. A. Wesson

Citation: Phys. Plasmas **3**, 3619 (1996); doi: 10.1063/1.871954
View online: http://dx.doi.org/10.1063/1.871954
View Table of Contents: http://pop.aip.org/resource/1/PHPAEN/v3/i10
Published by the American Institute of Physics.

Non-uniform rotation and the resistive wall mode

C. G. Gimblett
UKAEA, Fusion (UKAEA/Euratom Fusion Association), Culham, Abingdon Oxon, OX14 3DB, United Kingdom

R. J. Hastie, R. A. M. Van der Linden, and J. A. Wesson
JET Joint Undertaking, Abingdon, Oxon, OX14 3EA, United Kingdom

(Received 9 November 1995; accepted 26 June 1996)

Advanced Tokamak Concepts [C. Kessel, J. Manickam, G. Rewoldt, and W. M. Tang, Phys. Rev. Lett. **72**, 1212 (1994)] have been designed assuming that the ''Resistive Wall Mode'' (RWM) is stable. It has recently been shown that the RWM can be stabilized by a combination of strong uniform plasma rotation and visco-resistive dissipation. In this paper we examine the consequences of a sheared flow on the RWM, and contrast the results to the case of uniform flow. It is shown that, as for uniform flow, the rotation initially further destabilizes the resistive wall mode, but for higher rotation velocities the growth rate is reduced, and the presence of plasma dissipation may completely stabilize the mode. However, sheared rotation allows the possibility of the RWM coupling to and converting into a Kelvin-Helmholtz mode. It is shown that the position of the wall with respect to the critical position for stabilization of the external kink mode is of crucial importance. [S1070-664X(96)01010-5]

I. INTRODUCTION

There is much current interest in ''Advanced Tokamak Concepts.''[1] These devices aim at steady state operation with high β_p and strong bootstrap current. However, a consequence of this is that the broader current profiles are more susceptible to kink instabilities, with a consequent reduction in the β limit. Experimental evidence from the DIII-D tokamak,[2] however, indicates that β-driven kink modes are more stable than theoretically predicted.[3] This has lead to a reassessment of the theory of resistive wall modes, as it is clearly important to understand the fundamental physical processes which limit the achievable β.

The β values in advanced tokamak designs are constrained by low mode-number external kink instabilities. Ideal magnetohydrodynamic (MHD) theory predicts the existence of ideal external kink modes but also their stabilization by an infinitely conducting shell placed sufficiently close to the plasma. Allowing for the finite resistance of the vacuum vessel, further analysis shows that the instability appears as a ''resistive wall mode'' (RWM) growing on the characteristic flux diffusion time of the vessel. Furthermore, early analysis showed that the RWM was apparently unavoidable, with worrying implications for the performance of large toroidal devices with long pulse durations and the steady state operation of advanced tokamak concepts.

Indeed, thin-shell Reversed Field Pinch experiments seem to have verified the existence of these resistive wall modes, which can lead to termination of the discharge.[4,5] However, surprisingly, some tokamak plasmas appear to defy (by a significant factor) the β-limits predicted for the RWM,[3] behaving rather as if surrounded by a perfectly conducting shell. Such tokamaks are heated by the injection of neutral beams, which also impart strong plasma rotation. It is thought that plasma rotation may confer stability, introducing new physics into the theory of RWMs. Advanced tokamaks are currently being designed on the assumption that the resistive wall modes will be stable, but theoretical investigation as to why this may or may not be so, and how to optimize stability, is only just beginning.

It has been shown[6–8] that the RWM may be stabilized by a combination of strong plasma rotation and some form of plasma dissipation;[9] damping by the sound wave continuum in a cylinder,[7] or toroidal sideband coupling[6,7,10] or alternatively visco-resistive dissipation close to the plasma boundary.[8] These studies generally invoked uniform rotation, but strong recycling[11] at the tokamak edge should suppress the flow there and we may anticipate a strongly sheared flow. In this paper we employ a simple cylindrical model to examine the consequences of a sheared toroidal flow, in particular the presence of Kelvin-Helmholtz (K-H) like modes,[12] on the RWM. It should be stressed from the beginning that the objective is not to calculate the extent of the stability window between RWM and kink modes, a task which would require modelling both toroidal coupling effects and a specific damping mechanism (e.g., trapped ion collisional damping or ion Landau damping). Further, the presence of a separatrix could lead to significant changes.[13] The objective is rather to estimate at what values of plasma rotation velocity and shear the new K-H destabilizing mechanism makes a significant contribution within a simple cylindrical plasma model.

In Section II we outline the derivation of the governing equations and boundary conditions, and in Section III we investigate an analytic solution for a particular simple equilibrium. In Section IV we give the result of numerical solutions for more general field and rotation profiles, and this is followed by a discussion in Section V.

II. THE GOVERNING EQUATION AND BOUNDARY CONDITION

A. The governing equation

Our starting point is the linearized compressible MHD equations, including a mean flow **V**, i.e., the ideal induction equation,

$$\frac{\partial \mathbf{b}}{\partial t}=\nabla\times(\mathbf{v}\times\mathbf{B}+\mathbf{V}\times\mathbf{b}), \tag{1}$$

together with the equation of motion

$$\rho\left(\frac{\partial \mathbf{v}}{\partial t}+\mathbf{v}\cdot\nabla\mathbf{V}+\mathbf{V}\cdot\nabla\mathbf{v}\right)=-\nabla p+\mathbf{j}\times\mathbf{B}+\mathbf{J}\times\mathbf{b}, \tag{2}$$

and an adiabatic equation of state, which together with the mass continuity condition leads to

$$\frac{\partial p}{\partial t}+\mathbf{v}\cdot\nabla p_0+\mathbf{V}\cdot\nabla p=-\gamma p_0\nabla\cdot\mathbf{v}-\gamma p\nabla\cdot\mathbf{V}. \tag{3}$$

We employ a cylindrical coordinate system (r,θ,z) and take the equilibrium quantities (upper case in the equations above) to be $\mathbf{V}=V_0(r)\hat{\mathbf{z}}$ and $\mathbf{B}=(0,B_\theta(r),B_z(r))$ with $\mu_0\mathbf{J}=\nabla\times\mathbf{B}$. The equilibrium quantities of course obey the force balance equation

$$\rho(\mathbf{V}\cdot\nabla\mathbf{V})=-\nabla p_0+\mathbf{J}\times\mathbf{B}. \tag{4}$$

The perturbations (lower case in the above equations) are given exp $i(m\theta+kz-\omega t)$ dependencies and upon introducing the linearized Lagrangian displacement $\boldsymbol{\xi}$ with

$$\mathbf{v}=\frac{D\boldsymbol{\xi}}{Dt}=-i(\omega-\Omega(r))\boldsymbol{\xi}, \tag{5}$$

with $\Omega(r)=kV_0(r)$, we find that Eqs. (1)–(3) provide a complete set for the unknowns $b_r,b_\theta,b_z,\xi_r,\xi_\theta,\xi_z,p$ and can be reduced to a single governing equation for $\chi=r\xi_r$. This equation takes the form given in Ref. 7, but treats sheared toroidal flow. The equation was first derived in Refs. 14 and 15 which treated the general case of sheared toroidal and poloidal mass flows,

$$\frac{d}{dr}D(r)\frac{d\chi}{dr}-C(r)\chi=0, \tag{6}$$

where

$$D(r)=\rho\frac{(V_s^2+V_a^2)}{r}\frac{(\overline{\omega^2}-\omega_a^2)}{(\overline{\omega^2}-\omega_f^2)}\frac{(\overline{\omega^2}-\omega_h^2)}{(\overline{\omega^2}-\omega_s^2)}, \tag{7}$$

$$rC(r)=-\rho(\overline{\omega^2}-\omega_a^2)-\frac{4k^2V_a^2B_\theta^2}{\mu_0 r^2}\frac{(\omega_g^2-\overline{\omega^2})}{(\omega_f^2-\overline{\omega^2})}(\omega_s^2-\overline{\omega^2})+r\frac{d}{dr}\left[\frac{B_\theta^2}{\mu_0 r^2}+\frac{2kB_\theta G_0}{\mu_0 r^2}\frac{(V_s^2+V_a^2)}{(\omega_f^2-\overline{\omega^2})}\frac{(\overline{\omega^2}-\omega_h^2)}{(\overline{\omega^2}-\omega_s^2)}\right], \tag{8}$$

with $V_s^2=\gamma p_0/\rho$, $V_a^2=B^2/\mu_0\rho$, $\overline{\omega}=\omega-kV_0(r)$, $\omega_a=k_\parallel V_a(k_\parallel=F_0/B$ with $F_0=mB_\theta/r+kB_z)$, $\omega_h^2=\omega_a^2V_s^2/(V_s^2+V_a^2)$, $\omega_g=\omega_aV_s/V_a$, $\omega_{f,s}^2=\frac{1}{2}k_0^2(V_s^2+V_a^2)[1\pm\sqrt{1-\alpha^2}]$, $\alpha=2V_s\omega_a/k_0(V_s^2+V_a^2)$, $k_0^2=m^2/r^2+k^2$, and $G_0=mB_z/r-kB_\theta$.

As discussed in Ref. 7, if ω is real, Eq. (6) is singular at the radii where $\overline{\omega}=\omega_a$ (the Alfvén resonance) and $\overline{\omega}=\omega_h$ (the slow magnetosonic resonance). So, for a resistive wall mode with $\omega\sim0$ in the laboratory frame, plasma flows which are sonic $(\Omega\sim\omega_h)$ or Alfvénic $(\Omega\sim\omega_a)$ will introduce an element of continuum damping if the growth rate of the mode is small enough.[7]

However, for the tokamak application we have in mind there is very small separation in the frequencies ω_s and ω_h appearing in the numerator and denominator of $D(r)$,

$$\omega_s^2\sim\omega_h^2\left(1+\frac{k_\parallel^2V_s^2}{k_0^2V_a^2}\right)\sim\omega_h^2(1+\mathcal{O}(\epsilon^2\beta)), \tag{9}$$

with ϵ and β the inverse aspect ratio and ratio of plasma thermal to magnetic energies, respectively. Because of this, the closely paired zero and pole of the factor $(\overline{\omega^2}-\omega_h^2)/(\overline{\omega^2}-\omega_s^2)$ [which occur on the real r axis when the growth rate $\gamma=\mathcal{I}(\omega)=0$] move out into the complex r plane when $\gamma\neq0$ and effectively cancel when the condition,

$$\frac{\gamma}{\omega_s}>\left(1-\frac{nq}{m}\right)^2\frac{r^2}{R^2}\frac{V_s^2}{V_a^2}, \tag{10}$$

is satisfied [here R is the device major radius, $q=rB_z/(RB_\theta)$ is the safety factor and $n=kR$].

In this limit, then, we may employ the approximation $(\overline{\omega^2}-\omega_h^2)/(\overline{\omega^2}-\omega_s^2)\sim1$ and, making use of the standard tokamak expansion,[16] Eq. (6) may be put in the form

$$\frac{d}{dr}\left\{(1-A^2)r\frac{d\Psi}{dr}\right\}=\frac{m}{(m-nq)}\frac{r}{B_\theta}\frac{d}{dr}\left\{(1-A^2)J_z+2A^2\frac{B_\theta}{r}\right\}\Psi+\frac{m^2}{r}(1-A^2)\Psi, \tag{11}$$

where we have used a new dependent variable $\Psi=rb_r$ and

$$A^2\equiv\frac{\mu_0\rho\overline{\omega^2}r^2}{B_\theta^2(m-nq)^2}\equiv\left(\frac{\overline{\omega}}{\omega_a}\right)^2. \tag{12}$$

When plasma inertia is neglected $(\rho\to0)$ Eq. (11) is immediately recognized as the equation governing kink/tearing modes in a large aspect ratio tokamak.[16] From the above discussion we see that Eq. (11) applies to rotating plasmas with sheared flow $(d\Omega/dr\neq0)$ in both the subsonic and transonic limits, provided that the growth rate of any eigensolution satisfies inequality (10). For the moment we assume that the resistive wall time $\tau_W=b\delta/(2\eta)$ (b,δ, and η are the wall radial position, thickness, and resistivity, respectively) is such that (10) is satisfied when $\gamma\tau_W\leqslant1$, i.e., that

$$\omega_s\tau_W\ll\left(1-\frac{nq}{m}\right)^2\frac{r^2}{R^2}\frac{\mu_0\gamma p_0}{B_z^2}. \tag{13}$$

However when the growth rate of the RWM, calculated using Eq. (11), is depressed to such a low level that inequality (10) is no longer satisfied then the role of the sound resonance can no longer be neglected and continuum damping may then stabilize the mode, as shown in Ref. 7.

B. Boundary condition

The plasma has a free boundary at $r=a$. The boundary condition there is obtained by integrating Eq. (11) across a finite width plasma-vacuum interface and taking the zero width limit. We then find (a_- and a_+ subscripts denote plasma and vacuum, respectively)

$$\left(\frac{r}{\Psi}\frac{d\Psi}{dr}\right)_{a_+}=\left\{(1-A^2)\left(\frac{r}{\Psi}\frac{d\Psi}{dr}\right)\right\}_{a_-}-\frac{m}{(m-nq_a)}\frac{a}{B_{\theta a}}\left\{(1-A^2)J_z+2A^2\frac{B_\theta}{r}\right\}_{a_-}. \tag{14}$$

We now turn to the outer region and place a resistive wall at $r=b$, so there is vacuum for $a<r<b$ and $r>b+\delta$ where δ is the thickness of the wall. In the vacuum the solutions for Ψ are a linear combination of r^m and r^{-m} and the boundary condition at the wall (subscript W) is given by Ref. 17,

$$\left[\frac{r}{\Psi}\frac{d\Psi}{dr}\right]_W=-2i\omega\tau_W,$$

where $[\cdot]_W$ denotes the difference between the value on the two sides of the wall. Using this relation we can calculate the value of $(r/\Psi)d\Psi/dr$ at $r=a_+$ required in Eq. (14) and find[18]

$$\left(\frac{r}{\Psi}\frac{d\Psi}{dr}\right)_{a_+}=-m\frac{\{1+f(a/b)^{2m}\}}{\{1-f(a/b)^{2m}\}}, \tag{15}$$

where

$$f=\left(1+\frac{im}{\omega\tau_W}\right)^{-1}.$$

Equation (14), combined with (15), provides the boundary condition on Ψ at $r=a$.

III. AN ANALYTIC EXAMPLE

An analytic dispersion relation can be obtained from the equations formulated in section II above for the case of the simple, constant q, equilibrium $\mathbf{B}\equiv(0,B_{\theta0}(r/a),B_{z0})$, with $B_{\theta0}$ and B_{z0} constant. This example helps to isolate some generic properties of a sheared flow system.

A sheared flow is simulated by taking

$$\begin{aligned}\Omega&=\Omega_0, \quad 0\leqslant r\leqslant r_0,\\ &=\Omega_1, \quad r_0\leqslant r\leqslant a.\end{aligned} \tag{16}$$

For this case the quantity

$$A=\frac{(\omega-\Omega)}{\omega_A(m-nq)} \tag{17}$$

in Eq. (11) is a step function, having constant values on either side of r_0 [we have introduced the Alfvén frequency $\omega_A=B_{\theta0}/(a\sqrt{\mu_0\rho})$ based on the poloidal field at the plasma-vacuum interface]. The rotation profile of Eq. (16) introduces a discontinuity in $d\Psi/dr$ at r_0 and by integration of Eq. (11) through r_0 we obtain the jump condition

$$(1-A_0^2)\left(\frac{d\Psi}{dr}\right)_{r_{0_-}}=(1-A_1^2)\left(\frac{d\Psi}{dr}\right)_{r_{0_+}}, \tag{18}$$

where

$$A_j\equiv\frac{(\omega-\Omega_j)}{\omega_A(m-nq)}, \quad j=0,1, \tag{19}$$

for this particular equilibrium profile. Further, Eqs. (14) and (15) give

$$\left\{(1-A_1^2)\left(\frac{r}{\Psi}\frac{d\Psi}{dr}\right)\right\}_p=-m\frac{\{1+f(a/b)^{2m}\}}{\{1-f(a/b)^{2m}\}}+\frac{2m}{(m-nq)}, \tag{20}$$

as the relevant boundary condition at $r=a$. The solutions of the simplified Eq. (11) for Ψ are

$$\Psi=r^m; \quad 0<r<r_0, \tag{21}$$

$$=\alpha r^m+\beta r^{-m}; \quad r_0<r<a. \tag{22}$$

Using Eqs. (18) and (20) we can solve for the constants α and β and deduce the (in general quintic) dispersion relation,

$$(x^2+K-1)(x_0^2-2xx_0+2x^2-2)+\lambda x_0(x^2-K-1)(x_0-2x)=0, \tag{23}$$

where we have written

$$x=\frac{\omega-\Omega_1}{\omega_A(m-nq)}, \qquad x_0=\frac{\Omega_0-\Omega_1}{\omega_A(m-nq)},$$

$$\lambda=\left(\frac{r_0}{a}\right)^{2m},$$

and

$$K(\tau_W)=\frac{2}{(m-nq)}-\frac{\{1+f(a/b)^{2m}\}}{\{1-f(a/b)^{2m}\}}. \tag{24}$$

We choose to isolate $K(\tau_W)$ in this way because, for future reference, in the case of an ideally conducting wall ($\tau_W\to\infty, f\to1$) and no plasma rotation, the marginally stable wall position, b_c, is given by $K(\infty)=1$ or

$$\frac{2}{(m-nq)}-\frac{\{1+(a/b)^{2m}\}}{\{1-(a/b)^{2m}\}}=1, \tag{25}$$

i.e., b has to be sufficiently close to a.[19] That $K(\infty)=1$ gives the marginal point of the external kink is most easily seen by taking the case of zero rotation ($x_0=0$) in Eq. (23), which then becomes a quartic, and we find the four solutions,

$$x=\pm\sqrt{1-K(\infty)} \quad \text{and} \quad \pm1. \tag{26}$$

So provided $K(\infty)>1$ the system exhibits the well-known external kink mode with growth rate $\gamma=\sqrt{|K(\infty)-1|}$ (plus a stable complex conjugate counterpart), accompanied by two Alfvén waves. [Note that here and for the rest of this section we normalize all growth rates and frequencies to $(m-nq)\omega_A$.] An equivalent way of obtaining the ideal kink is to take $r_0=a$, i.e., $\lambda=1$. Equation (23) then factorizes to give the same roots as discussed above.

We now investigate the effect of rotation on the position of this marginal point. It is easy to see that uniform rotation ($\Omega_0=\Omega_1$, i.e., $x_0=0$) leaves Eq. (26) unaltered and the marginal point unchanged. For the case of sheared rotation we take as an example $m=2$ and $nq=1.5$, so the kink is marginally stable for a wall at $(a/b)^{2m}=0.5$. Now, placing the velocity shear layer at $(r_0/a)^{2m}=0.8$ we leave Ω_1 at 0, in-

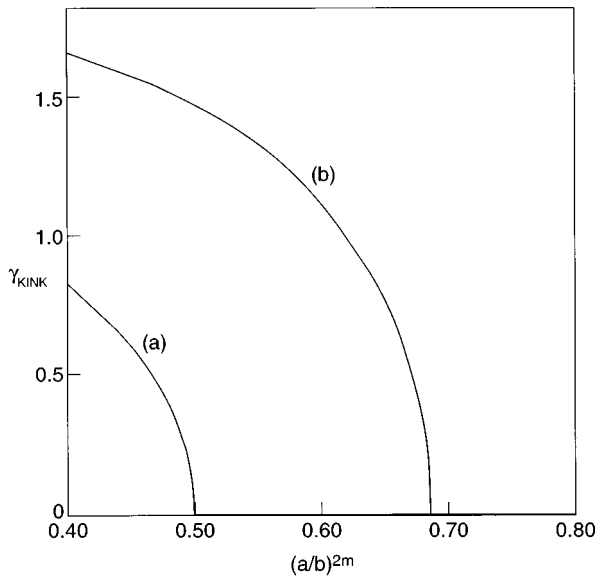

FIG. 1. The growth rate of the ideal kink mode as the wall is moved from outside the marginal point to inside $[(a/b)^{2m}$ going from 0.4 to 0.8]. (1a) is the non-rotating and (1b) the sheared rotation case. We see that sheared rotation has the effect of further destabilizing the external kink by moving the position of the marginal point from $(a/b)^{2m}=0.5$ to ~ 0.69, i.e., the wall has to be placed nearer to the plasma to give marginal stability. [Parameters: $m=2$, $nq=1.5$, $(r_0/a)^{2m}=0.8$, $(a/b)^{2m}=0.4-0.8$, $\Omega_0=0(1a)$, $5(1b)$, $\Omega_1=0$, $\tau_W\rightarrow\infty$.]

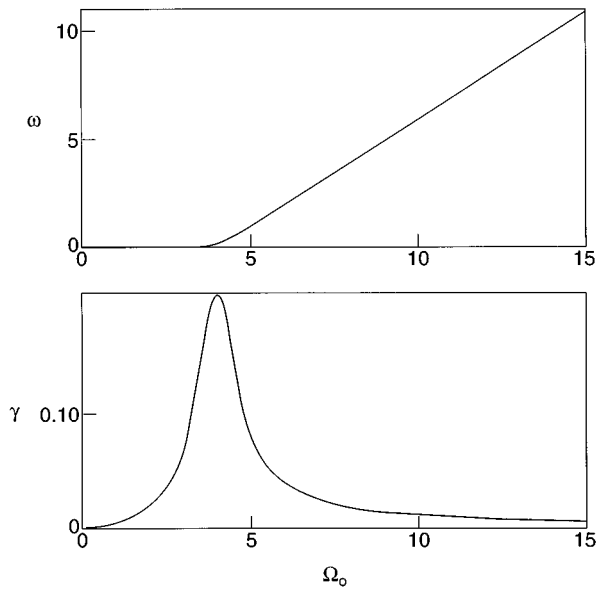

FIG. 2. The real and imaginary parts of the RWM ω versus rotation frequency. As the rotation is increased the growth rate initially also increases, while the mode remains locked to the wall, but at $\Omega_0\sim 4$ the mode starts to slip relative to the wall and the growth rate $\rightarrow 0$ while never completely stabilizing. [Parameters : $m=2$, $nq=1.5$, $(r_0/a)^{2m}=1.0$, $(a/b)^{2m}=0.9$, $\Omega_0=0-15$, $\Omega_1=0$, $\tau_W=500$.]

crease Ω_0 to 5, and ask what effect this has on the kink mode. Figure 1 shows the growth rate of the mode as the wall is moved from outside the marginal point to inside $[(a/b)^{2m}$ going from 0.4 to 0.8]. Figure 1(a) is the non-rotating and (1b) the sheared rotation case. We see that in the latter case the external kink is further destabilized in that the marginal point is moved from $(a/b)^{2m}=0.5$ to ~ 0.69, i.e., the wall has to be placed nearer to the plasma to give marginal stability.

Staying with the case of a perfect wall, an interesting situation occurs when we put the wall directly on the plasma. Then $K(\infty)\rightarrow\infty$ and Eq. (23) gives

$$\omega=\frac{1}{2}[(\Omega_0+\Omega_1)+\lambda(\Omega_1-\Omega_0)]$$

$$\pm\frac{1}{2}\sqrt{(\lambda^2-1)(\Omega_0-\Omega_1)^2+4}. \tag{27}$$

Accordingly, this root is Doppler shifted to a λ-weighted mean of Ω_0 and Ω_1 and becomes unstable for sufficient velocity shear, i.e., when

$$|\Omega_0-\Omega_1|>\frac{2}{\sqrt{1-\lambda^2}}. \tag{28}$$

We identify this mode as a Kelvin-Helmholtz (K-H) instability,[12,20] although as we discuss below the nomenclature and identification of kink, K-H and RWM is in general not a simple affair. Note that the K-H instability of Eq. (27) remains present for $\lambda\rightarrow 0$ but not for $\lambda\rightarrow 1$.

We now reinstate the finite conductivity of the wall and can isolate the RWM in Eq. (23) by, say, taking $\lambda\rightarrow 0$. This leaves only the first term of Eq. (23); the second bracket of this term gives the KH mode while the first, i.e., x^2+K-1 gives the kink/RWM branch. To see this clearly we take inertia to be negligible $(x=0)$ and find the solution

$$\omega\tau_W=\frac{2im\Gamma}{(a/b)^{2m}-\Gamma},\qquad \Gamma=1-m+nq. \tag{29}$$

This, then, is the RWM for $0<\Gamma<(a/b)^{2m}$ which converts to the external kink for $\Gamma\geqslant(a/b)^{2m}$. But this is precisely the condition $K(\infty)=1$ of Eq. (25). In other words, we have the well-known statement that the RWM only exists in conditions where the external kink mode would be unstable were there no wall at all and the resistive wall is placed within the marginally stable position for that mode.

If we take into account finite inertia in this case then under uniform rotation of the plasma the RWM exhibits the characteristic behavior found in Ref. 17. This feature is reproduced in Fig. 2 where we show the dependence of the real and imaginary parts of ω on the (uniform) rotation velocity. We see that as the rotation is increased the growth rate initially also increases, while the mode remains locked to the wall, but at $\Omega_0\sim 4$ the mode starts to slip relative to the wall and the growth rate asymptotes to zero as the rotation velocity tends to infinity. Complete stability is not obtained for finite rotation. Note that the rotation velocities here are all normalized by the quantity $(m-nq)$, which is characteristically small at the plasma edge for the external kink, and so the rotation required to produce $\gamma\rightarrow 0$ in the tokamak case is proportionately smaller than Alfvénic (see also section V below).

We now turn to the case of the RWM in the situation of sheared rotation. Again we take $m=2$,$nq=1.5$, which im-

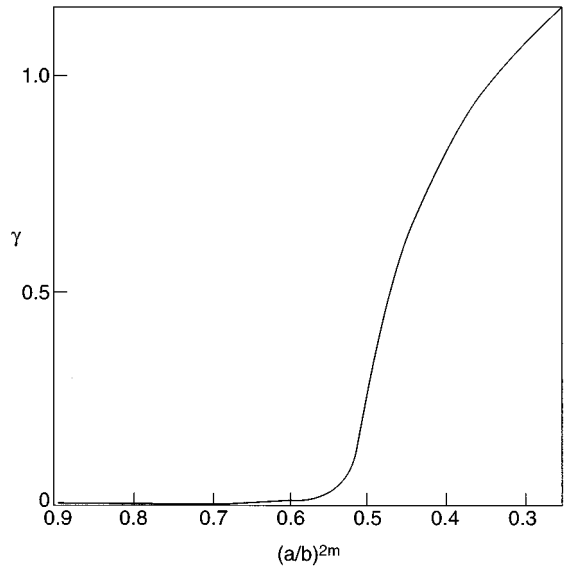

FIG. 3. The growth rate of the RWM converts to that of the ideal external kink as the wall moves through the marginal position for the ideal kink. [Parameters: $m=2$, $nq=1.5$, $(r_0/a)^{2m}=1.0$, $(a/b)^{2m}=0.9-0.25$, $\Omega_0=0$, $\Omega_1=0, \tau_W=500.$]

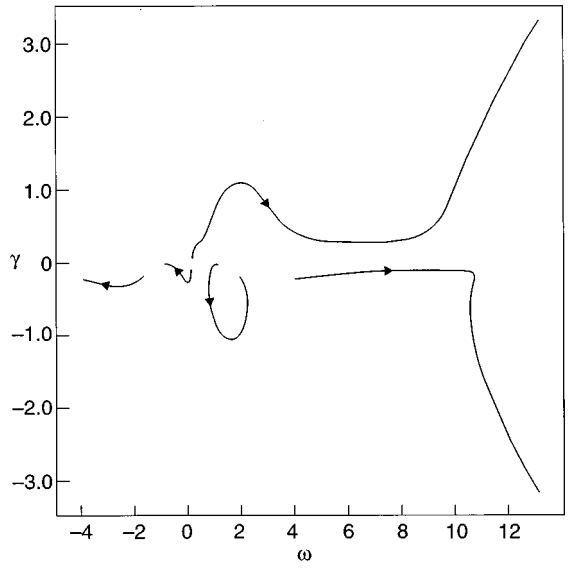

FIG. 4. The locus of the five solutions of Eq. (23) in the complex plane as Ω_0 is taken from zero to 15. The RWM, originally located at (0.0,0.05), initially shows the same behavior as a RWM subject to uniform rotation[17] but eventually converts to a strong Kelvin-Helmholtz like instability. The four Alfvén waves remain damped. [Parameters: $m=2$, $nq=1.5$, $(r_0/a)^{2m}=0.75, (a/b)^{2m}=0.9$, $\Omega_0=0-15$, $\Omega_1=0, \tau_W=50.$]

plies that the kink mode is marginally stable for an ideal wall at $(a/b)^{2m}=0.5$; we ensure that we are studying a RWM by taking $(a/b)^{2m}=0.9$. In fact Fig. 3 shows the growth rate of the RWM converting to that of the kink as the wall is moved from inside this point to outside it. In this case we have taken $\tau_W=500$ so that γ converts from the RWM growth rate $\sim 10^{-3}$ to the kink (~ 1) as the wall moves through the critical value of 0.5. To increase the RWM growth rate we now take $\tau_W=50$ and introduce a velocity shear at $(r_0/a)^{2m}=0.75$. When the plasma is at rest we find the five roots of the quintic [Eq. (23)] are at $(\Omega,\gamma)=(0.0,0.05)$, $(\pm 1,0.0)$, and $(\pm 4, -0.0225)$. The first is the RWM, the next two are two undamped Alfvén waves associated with the plasma itself, while the last two are plasma Alfvén waves that are damped due to interaction with the wall. If we now keep Ω_1 at zero but increase the rotation of the core, Ω_0, we can find the locus of these roots in the imaginary plane and this is shown in Fig. 4. The RWM, originally located at (0.0,0.05) initially shows the same behavior as a RWM subject to uniform rotation.[17] That is, there is an initial further destabilization of the mode but at $\gamma\sim 1$ this ceases and the growth rate decreases. However, unlike the case of uniform rotation, at $\omega\sim 9$ the mode is strongly destabilized and has converted to a K-H-like instability. The four Alfvén waves remain damped.

IV. NUMERICAL RESULTS

We now turn to numerical solutions of Eq. (11) for general non-uniform rotation frequencies. These solutions were obtained using finite differences with variable grid spacing and Newton iteration.

In all numerical results discussed here we used the following class of magnetic equilibria:

$$j_z=j_o\left(1-\frac{r^2}{a^2}\right)^{\nu}, \tag{30}$$

$$B_\theta=\frac{j_o}{2r(\nu+1)}[1-(1-r^2)^{\nu+1}]. \tag{31}$$

All distances are scaled to the plasma minor radius a (a dimensionless coordinate $x\equiv r/a$ is introduced), and time is scaled to the resistive wall time [in the Joint European Torus (JET) tokamak,[21] $\tau_W\approx 4\times 10^{-3}$ s].

A. Comparison with analytic model

To compare with the solutions obtained using the analytic model we used a rotation profile described by

$$2\Omega=(\Omega_0+\Omega_1)+(\Omega_0-\Omega_1)\tanh[\lambda_\Omega(x_0^2-x^2)]. \tag{32}$$

For λ_Ω tending to infinity this function tends to a Heaviside step function. Results obtained with the numerical code for large λ_Ω have been compared with the analytic results and show good agreement. This is illustrated in Fig. 5 for a typical case. Using an ideal wall rather than a resistive one, two unstable modes are present: an external kink and a K-H instability (as has been noted there is not always a complete and clear distinction between these two modes). In this case, the external kink growth rate is almost unaffected by the rotation and its frequency is practically identical to the rotation frequency in the outer part of the plasma. The K-H mode frequency is an average of the rotation frequency over the plasma, while its growth rate depends strongly on the shear in the flow.

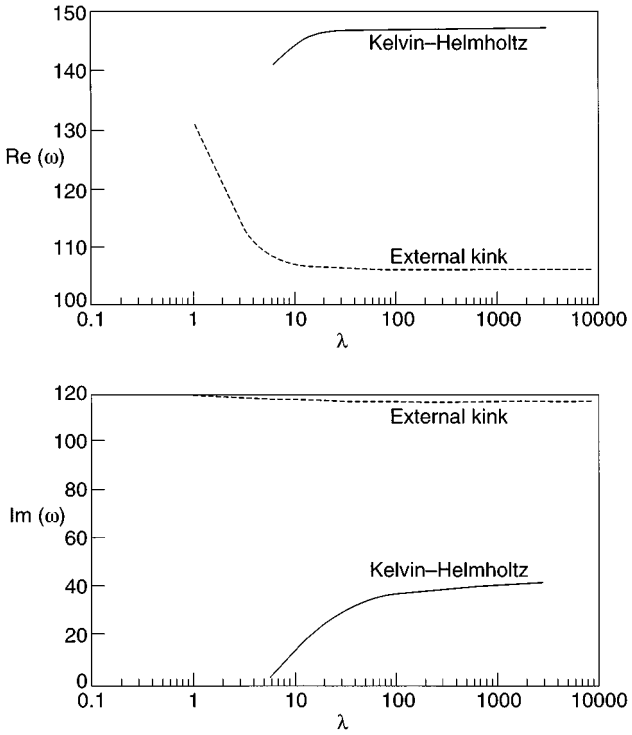

FIG. 5. Frequency and growth rate of the ''external kink'' (dashed line) and ''Kelvin-Helmholtz'' (full line) type modes versus the parameter λ_Ω regulating the sharpness of the step-like tanh rotation frequency profile (32) approximating the analytical model. Equilibrium parameters are $\Omega_0=200$, $\Omega_1=100$, $x_0/a=0.5$, $a/b=0.9$, $m=2$, $m-nq_a=0.1$, $\tau_A/\tau_W=10^{-3/2}$.

B. A comparison of uniform and sheared toroidal rotation

We now turn to more realistic profiles for the equilibrium quantities. In the first instance we take the equilibrium profiles (30), (31) with $\nu=1$ and a uniform toroidal rotation frequency:

$$\Omega=\omega_0. \tag{33}$$

For the equilibrium parameters selected in Fig. 6, the ideal external kink then becomes stable at a critical distance of the wall given by $(a/b)_c\approx 0.9017$. With a resistive wall placed inside this position there is a remnant RWM instability, its growth rate depending on the wall position. As the plasma is given a certain rotation, the well-known typical curves for growth rates and frequencies are obtained, as illustrated in Fig. 6. For low rotation rates the mode remains locked to the wall, and the mode frequency remains small compared to the rotation frequency. In this regime the wall remains an ineffective conductor and consequently the rotation cannot have any stabilizing influence. On the contrary, the growth rate increases if the wall is sufficiently close to the plasma (this effect being due to the plasma-wall interaction). From a certain critical rotation rate, the mode breaks away from the wall and the wall starts to act as an increasingly good conductor, thus reducing the growth rate. For all wall distances (inside the critical distance for the onset of the external kink), the growth rate asymptotes to zero as the rotation rate tends to infinity. In a more complete treatment, this residual growth rate may be removed by dissipative effects.[6–8] Since the required rotation rate increases as the wall distance decreases, it has been argued that the optimum position of the wall for a given configuration is just inside the position where the ideal kink would set in.

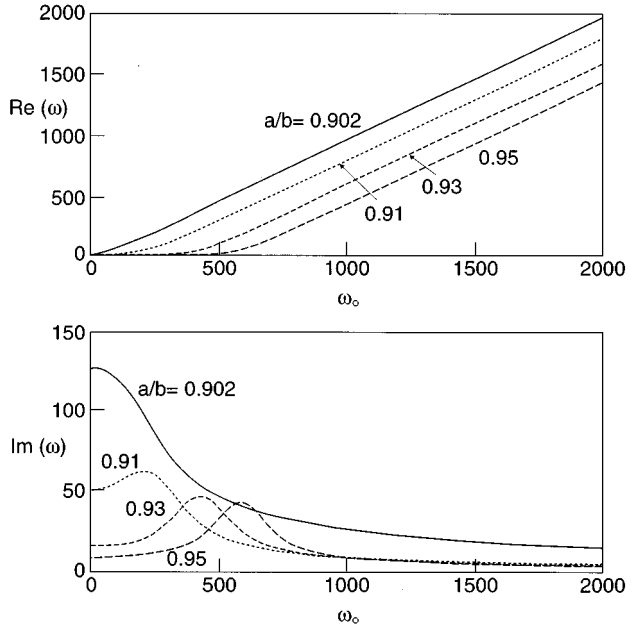

FIG. 6. Frequency and growth rates of the $m=2$ resistive wall mode versus (uniform) rotation frequency for different positions of the wall (values of a/b are indicated on the figure). Time is scaled to the resistive wall time. The equilibrium has $m-nq_a=0.1$, $\nu=1.0$, $\tau_A/\tau_W=1.5\times10^{-4}$.

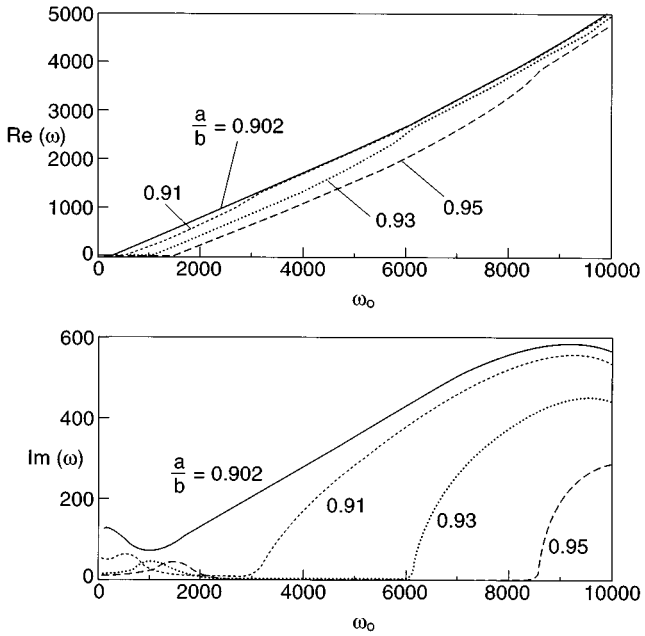

FIG. 7. The same as in Fig. 6 with the same equilibrium, but now using a sheared rotation profile given by Eq. (34). The pedestal value was always taken to be 0.4 times the amplitude of the parabolic component: $\omega_b=0.4\omega_0$.

This statement needs to be reconsidered however when a sheared rotation is included, as is demonstrated in Fig. 7. Here, we have introduced the profile

$$\Omega = \omega_0(1-x^2) + \omega_b\,, \tag{34}$$

which agrees reasonably with the experimental profiles. In Fig. 7 the pedestal value ω_b was set at 0.4 times the amplitude of the parabolic component, which again is typical for experimental rotation profiles. It is apparent that for low rotation frequencies the results are qualitatively identical to the case of uniform rotation. When the rotation rate becomes high enough however, the mode switches to the K-H instability, and the growth rate starts to increase again. The turn-up of the growth rate occurs for *lower* rotation rates as the wall distance is increased. Hence, the optimum wall distance is probably no longer given by the same value as that for the uniform rotation case, since for this wall distance the K-H instability may increase the growth rate before it has been reduced to low enough values to be stabilized by dissipation. This statement requires further verification in a more complete analysis.

It can be argued that toroidal effects may be partly represented in cylindrical geometry by an increase in the effective inertia,[22] with $\rho \to \Lambda\rho$, $\Lambda \gg 1$ in the inertial ''layer'' near the plasma boundary where $m - nq \ll m$. In a collisional plasma the enhanced inertia arises from the large longitudinal displacements $\xi_\parallel$ which are required by the dual constraints of incompressibility $\nabla \cdot \boldsymbol{\xi} = 0$ and vanishing magnetic compression $\mathbf{B} \cdot \delta\mathbf{B} \approx 0$. In toroidal geometry these constraints require the existence of $m \pm 1$ side-band harmonics in $\xi_\parallel$ with

$$\xi_\parallel \approx q\,\xi_{\perp\theta}\,, \tag{35}$$

so that $\Lambda = 1 + 2q^2$. A similar inertial enhancement is predicted[23] in the banana regime of collisionality with $\Lambda = 1 + 1.6q^2/\epsilon^{1/2}$ where $\epsilon = r/R_0$. To model this effect we have considered the case of a ten times higher density, which reduces the Alfvén time scale by a factor of $\sqrt{10}$. This is represented in Figs. 8 and 9. The main change is that the scale of the graph is condensed by the same factor. Thus the onset of the shear flow driven instability now occurs for $\omega_0 \simeq 2700$ instead of $\omega_0 \simeq 8600$ (for the case $a/b = 0.95$). At values of ω_0 greater than this the instability persists if the resistive wall is replaced by a perfectly conducting wall, i.e., the terminology ''resistive wall mode'' is no longer appropriate, and we should refer to the mode as a shear flow driven mode of K-H character. As ω_0 is increased beyond the K-H threshold the growth rate rises to a maximum (at $\omega_0 \simeq 3200$ in the case of $a/b = 0.95$) before decreasing again. This behavior is caused by Alfvén continuum damping. At $\omega_0 \simeq 3200$ an Alfvén resonance, $\mathcal{R}e(\omega) = (m - nq)V_A/Rq$ enters the plasma at the plasma boundary. In Fig. 9 we also include a repeat of the calculation for $a/b = 0.95$, but with the pedestal value of the rotation frequency removed, so that the edge rotation is always zero. This substantially changes the results. The mode remains locked to the wall for much higher values of the central rotation frequency, and the growth rate curve no longer displays the initial increase and fall-off before the K-H instability takes over. It is also of interest to note that once the K-H is dominant, the two curves for $a/b = 0.95$ coincide, indicating that the growth rate is only determined by the total amount of shear in the rotation profile, and not by the uniform contribution to the rotation profile.

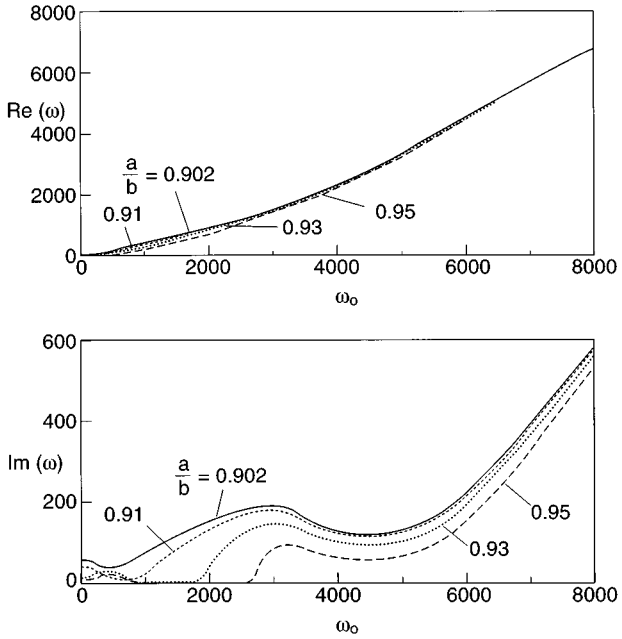

FIG. 8. As in Fig. 7 with a ten times larger value for the ratio τ_A^2/τ_W^2, modelling toroidal enhancement of inertia.

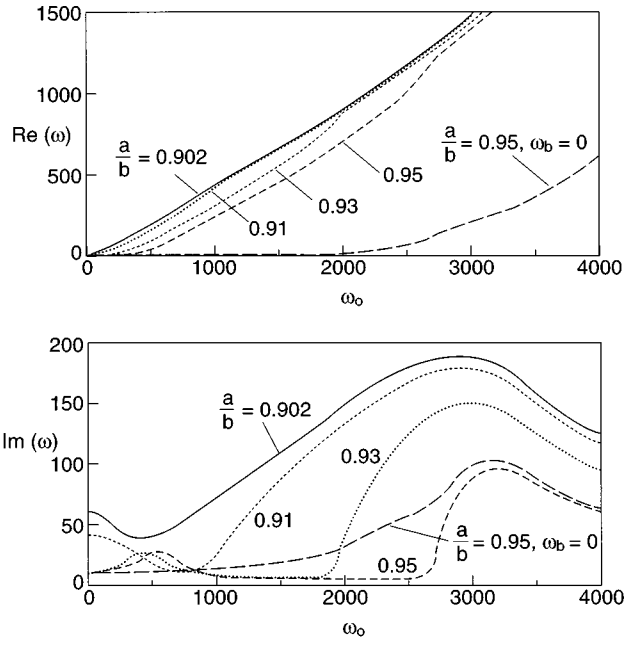

FIG. 9. An enlargement of the low rotation frequency part of Fig. 8. Also included are curves for the case with $a/b = 0.95$ and the pedestal in the rotation profile removed, so that the rotation frequency drops to zero at the edge of the plasma ($\omega_b = 0$).

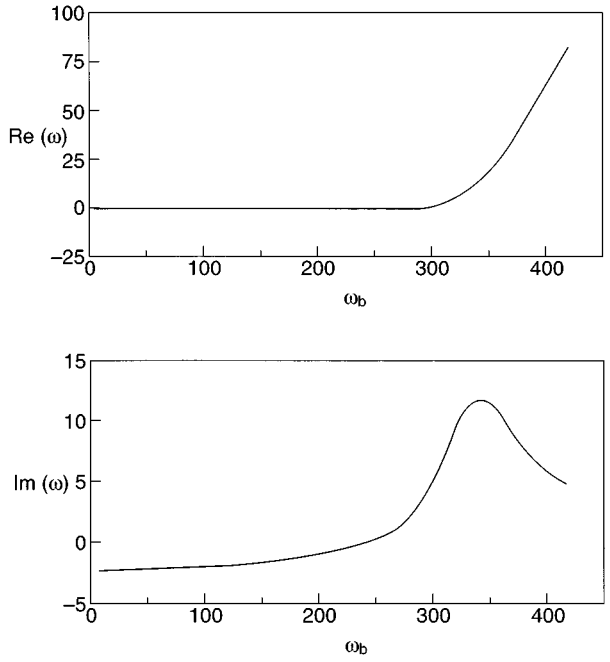

FIG. 10. Growth rate and frequency of the resistive wall mode versus *edge* rotation frequency in a JET model equilibrium. We have used $\tau_A/\tau_W = 1.7\times 10^{-4}$, $b/a = 1.2$, $\nu = 2$, $m = 3$, $m - nq_a = 0.1$. The rotation profile is again given by Eq. (34) with $\omega_b = 0.4\omega_0$.

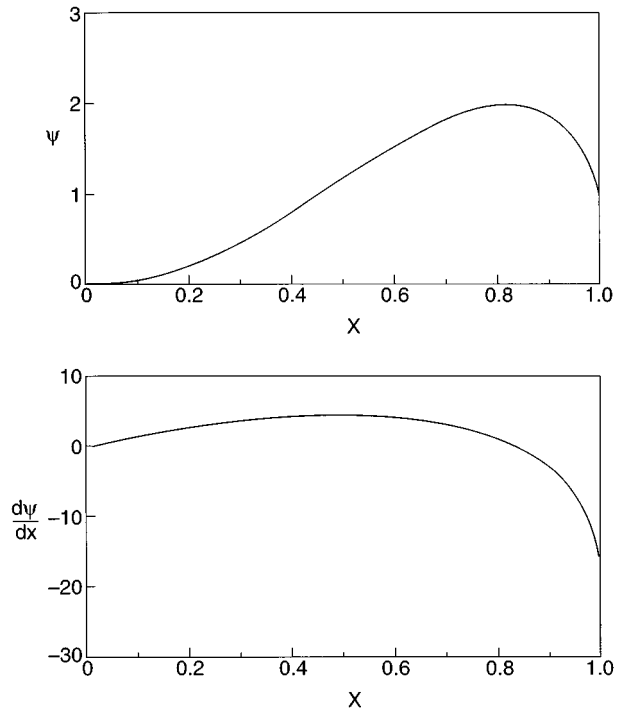

FIG. 12. Typical eigenfunctions (top) and the first derivative for the cases presented in Figs. 10 and 11.

C. Relevance for JET

A more meaningful model equilibrium is obtained for JET by taking $\nu = 2$ in the magnetic profiles. Typical values for the rotation frequency are $\Omega\tau_W = 280$ and $\omega_b\tau_W = 80$. For the JET model values adopted in Figs. 10 and 11 for the various other parameters it turns out that there is no external kink instability (for *any* wall distance) in the zero-pressure approximation (to include pressure in a realistic way would require a fully toroidal calculation). Therefore, the RWM in the absence of toroidal rotation is a purely damped mode. As has already been pointed out in Ref. 17 however, this mode can still be driven unstable when rotation is included, as demonstrated in Fig. 10 for the sheared rotation profile, and in Fig. 11 for uniform rotation. (In both cases the growth rates are plotted versus the edge rotation frequency). For the quoted typical edge rotation rate for JET, the mode is still damped for both figures. However, there is only a factor 2 to 3 difference between a typical rotation rate in JET and the value required to obtain an instability in our model. In view of the simplicity of the model and the above reference to enhanced inertial effects and other toroidal corrections, there is a definite possibility that the RWM instability may be of relevance in the JET experiments.

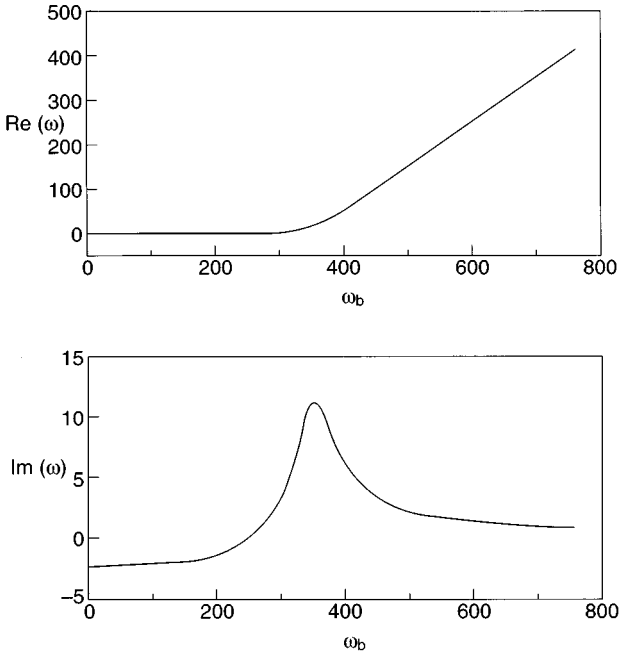

FIG. 11. The same as in Fig. 10 with the same equilibrium, but taking uniform rotation.

For completeness, in Fig. 12 we present a typical eigenmode structure corresponding to a low rotation frequency point in Fig. 10. This eigenfunction still has all the characteristics an external kink mode would have. We should point out however that the eigenfunctions may become severely distorted in several ways, in particular when substantial interaction with the Alfvén resonance is present.

V. CONCLUSIONS AND DISCUSSION

In this paper we have concentrated on the effects of sheared toroidal rotation on the external kink resistive wall mode (RWM). It is known that uniform rotation produces an initial further destabilization of the mode but at higher rotation rates the growth rate asymptotes to zero (but never ac-

tually stabilizes). It is known that plasma rotation coupled with some form of plasma dissipation,[9] either a visco-resistive outer plasma region[8] or damping on the sound continuum[6,7] can bring about complete stabilization of this reduced growth rate. However, the stability window (i.e., the range in value of b/a for which the RWM is stable) which results from either of these mechanisms appears to be very small in the cylindrical models.

When toroidal momentum is injected into a tokamak plasma the edge rotation is limited by momentum loss through rapid recycling at the plasma surface, and consequently the toroidal flow will be radially sheared. We have investigated a simple analytic case, and a more general numerical formulation, of a model that incorporates the effects of sheared flow and find that the growth rate of the RWM does not always asymptote to zero but can couple with and transform into a Kelvin-Helmholtz (K-H) type instability.[12] In this case the question of the optimum wall distance for stabilizing the RWM may need to be reconsidered.

We have noted that the plasma velocity only appears in our calculations normalized by $(m-nq)v_A$. Now $(m-nq)$ is typically a small quantity (at least at the plasma edge) for the external kink in a tokamak. Secondly, the toroidal enhancement of inertia discussed in section IV has the effect of decreasing v_A. As a result the actual plasma velocity required to produce the various phenomena discussed in this paper is significantly less than might be expected. As an example we showed that for typical JET parameters, although the RWM is stable for zero rotation, the effect of plasma flow may be sufficient to destabilize it.

The presence of the K-H mode at higher sheared rotation naturally leads to speculation regarding the role of this mode in the phenomenon of ''roll over'' observed in several experiments, as well as its implications for edge localized modes (ELMs).[20]

ACKNOWLEDGMENTS

We thank C. N. Lashmore-Davies for discussions.

This work was funded jointly by the U.K. Department of Trade and Industry and EURATOM.

[1] C. Kessel, J. Manickam, G. Rewoldt, and W. M. Tang, Phys. Rev. Lett. **72**, 1212 (1994).
[2] T. S. Taylor, E. A. Lazarus, M. S. Chu, J. R. Ferron, F. J. Helton, W. Howl, G. L. Jackson, T. H. Jensen, Y. Kamada, A. G. Kellman, L. L. Lao, R. J. La Haye, J. A. Leuer, J. B. Lister, T. H. Osborne, R. Snider, R. D. Stambaugh, E. J. Strait, and A. D. Turnbull, in *Plasma Physics and Controlled Nuclear Fusion Research 1990*, Proceedings of the 13th International Conference, Washington, DC (International Atomic Energy Agency, Vienna, 1991), Vol. 1, p. 177.
[3] E. J. Strait, T. S. Taylor, A. D. Turnbull, J. R. Ferron. L. L. Lao, B. Rice, O. Sauter, S. J. Thompson, and D. Wròblewski, Phys. Rev. Lett. **74**, 2483 (1995).
[4] B. Alper, M. K. Bevir, H. A. B. Bodin, C. A. Bunting, P. G. Carolan, J. Cunnane, D. E. Evans, C. G. Gimblett, R. J. Hayden, T. C. Hender, A. Lazaros, R. W. Moses, A. A. Newton, P. G. Noonan, R. Paccagnella, A. Patel, H. Y. W. Tsui, and P. D. Wilcock, Plasma Phys. Controlled Fusion **31**, 205 (1989).
[5] P. Greene and S. Robertson, Phys. Fluids B **5**, 556 (1993).
[6] A. Bondeson and D. J. Ward, Phys. Rev. Lett. **72**, 2709 (1994); D. J. Ward and A. Bondeson, Phys. Plasmas **2**, 1570 (1995).
[7] R. Betti and J. P. Freidberg, Phys. Rev. Lett. **74**, 2949 (1995).
[8] R. Fitzpatrick and A. Aydemir, Nucl. Fusion **36**, 11 (1996).
[9] M. S. Chu, J. M. Greene, T. H. Jensen, R. L. Miller, A. Bondeson, R. W. Johnson, and M. E. Mauel, Phys. Plasmas **2**, 2236 (1995).
[10] A. B. Mikhailovskii and B. N. Kuvshinov, Phys. Lett. A **209**, 83 (1995).
[11] G. P. Maddison, D. Reiter, P. C. Stangeby, and A. K. Prinja, in *Proceedings of the 20th EPS Conference on Controlled Fusion and Plasma Physics*, Lisbon, 1993, European Physics Conference Abstracts (European Physical Society, Petit-Lancy, Switzerland, 1993), Vol. 17C, Part II, p. 779.
[12] S. Chandrasekhar, *Hydrodynamic and Hydromagnetic Stability* (Clarendon, Oxford, 1961).
[13] A. H. Boozer, Phys. Plasmas **2**, 4521 (1995).
[14] E. Hameiri, Ph.D. thesis, New York University, 1976.
[15] A. Bondeson, R. Iacono, and A. Bhattacharjee, Phys. Fluids **30**, 2167 (1987).
[16] J. A. Wesson, *Tokamaks* (Clarendon, Oxford, 1987).
[17] C. G. Gimblett, Nucl. Fusion **26**, 617 (1986).
[18] M. F. F. Nave and J. A. Wesson, Nucl. Fusion **30**, 2575 (1990).
[19] J. A. Wesson, Nucl. Fusion **18**, 87 (1978).
[20] H. R. Strauss, Nucl. Fusion **32**, 2021 (1992).
[21] P. H. Rebut and B. E. Keen, Fusion Technol. **11**, 1 (1987).
[22] A. H. Glasser, J. M. Greene, and J. L. Johnson, Phys. Fluids **19**, 567 (1976).
[23] A. B. Mikhailovskii and V. S. Tsypin, Sov. J. Plasma Phys. **9**, 91 (1983).